THROUGH WALL SURVEILLANCE USING ULTRAWIDEBAND RANDOM NOISE RADAR

C.P. Lai and R. M. Narayanan
The Pennsylvania State University
University Park, PA 16802

G. Culkowski
Acquisition Logic, Inc.
Chantilly, VA 20151

ABSTRACT

Recent terrorist activities and law-enforcement situations involving hostage situations underscore the need for effective through-wall detection. Current building interior imaging systems are based on short-pulse waveforms, which require specially designed antennas to subdue unwanted ringing. In addition, periodically transmitted pulses of energy are easily recognizable by the intelligent adversary who may employ appropriate countermeasures to confound detection. A non-coherent polarimetric random noise radar architecture is being developed based on ultrawideband (UWB) technology and software defined radio, which has great promise in its ability to covertly detect obscured targets. The main advantages of the random noise radar lie in two aspects: first, random noise waveform has an ideal "thumbtack" ambiguity function, i.e., its down range and cross range resolution can be separately controlled, thus providing unambiguous high resolution imaging at any distance; second, random noise waveform is inherently low probability of intercept (LPI) and low probability of detection (LPD), i.e., it is immune from detection, jamming, and interference. Thus, it is an ideal candidate sensor for covert imaging of obscured regions in hostile environments. Other than those advantages, we also suffer some real problems that we lack of the back scattering information in the strong clutter and interference environment and most of the previous through wall studies are based on the research of light cluttered environment. This paper presents the radar system design, simulation study, measurements, and data analysis.

1. INTRODUCTION

Through wall imaging technology has been developed for many years. In the late 80's, there was considerable research related to earthquake survivor search. The original idea was to detect the human heart beat and respiration by using a narrow band radar system (e.g., Popovic et al., 1984). The radar system was simple and contained simple digital signal processing technology. By the late 90's, Time Domain Corporation started their business to develop the first UWB through wall radar system. In parallel, the Department of Justice and the Department of Defense also conducted research on wall penetrating radar technology. Radar Vision II, released by Time Domain Corporation in 2005, has human tracking (moving and stationary person), standoff detection and some other advanced functions (Nag and Barnes, 2003). However, there are still many improvements that can be implemented in next generation radar systems, especially with regard to covertness of the transmit signal and immunity from interference and jamming.

Current through wall radars are short pulse systems which have the advantage of exact localization of a moving person or some slight human movements. However, its repeatable waveform characteristics will increase the detection probability by intelligent adversaries and expose the user's position. In order to covertly detect the human activities, an example of using a 250-500 MHz random noise radar system was studied for wall penetration imaging applications (Narayanan et al., 2004). The resulting images of the obscured trihedral reflector and other targets clearly demonstrate the good wall penetration imaging capability of the random noise radar system. Both UWB pulse radar and noise radar suffer from the problem of harsh indoor clutter that will make human target recognition difficult. Separation of stationary or slow-moving humans from strong clutter reflections is a difficult problem.

2. SOFTWARE DEFINED NOISE RADAR

2.1 System design

In the typical UWB noise radar system, use of conventional microwave component technology makes the unit heavy and inconvenient to deploy and operate in the field. The software defined radio (SDR) concept has provided a novel solution for advancing current technology to a new generation of systems that import appropriate digital techniques. The SDR concept, first proposed in 1989 (Tsui, 1989), has been widely used in new wireless technology, such as third generation mobile phone, global positioning systems (GPS), and other personal communication tools. SDR techniques have also provided new ideas for the design of modern radar systems that are reliable, compact, and light-weight (Wu and Li, 1998; Wiesbeck, 2001). Considerable improvement in system performance has been observed compared to conventional radar.

Report Documentation Page

Form Approved
OMB No. 0704-0188

1. REPORT DATE	2. REPORT TYPE	3. DATES COVERED
01 NOV 2006	**N/A**	**-**

4. TITLE AND SUBTITLE	5a. CONTRACT NUMBER
Through Wall Surveillance Using Ultrawideband Random Noise Radar	5b. GRANT NUMBER
	5c. PROGRAM ELEMENT NUMBER
6. AUTHOR(S)	5d. PROJECT NUMBER
	5e. TASK NUMBER
	5f. WORK UNIT NUMBER
7. PERFORMING ORGANIZATION NAME(S) AND ADDRESS(ES) **The Pennsylvania State University University Park, PA 16802**	8. PERFORMING ORGANIZATION REPORT NUMBER
9. SPONSORING/MONITORING AGENCY NAME(S) AND ADDRESS(ES)	10. SPONSOR/MONITOR'S ACRONYM(S)
	11. SPONSOR/MONITOR'S REPORT NUMBER(S)

12. DISTRIBUTION/AVAILABILITY STATEMENT
Approved for public release, distribution unlimited

13. SUPPLEMENTARY NOTES
See also ADM002075.

14. ABSTRACT

15. SUBJECT TERMS

16. SECURITY CLASSIFICATION OF:			17. LIMITATION OF ABSTRACT	18. NUMBER OF PAGES	19a. NAME OF RESPONSIBLE PERSON
a. REPORT	b. ABSTRACT	c. THIS PAGE			
unclassified	**unclassified**	**unclassified**	**UU**	**8**	

The model-based approach minimizes the differences between simulation and the measurement by using the SDR concept. Such architectures can be realized by powerful analog-to-digital converters (ADCs) and state-of-the-art digital signal processing technology. Unlike traditional radar systems, the radio frequency (RF) front-end circuits and analog delay lines can be replaced by digital integrated circuit components. The size and weight of the radar system can be reduced and power can be saved.

While radar technology is mature, implementation of short-pulse or wideband frequency-modulated radar systems is relatively expensive for through-wall surveillance (TWS) applications. Furthermore, such systems are easily detectable by today's techno-terrorists. To confound detection, ultrawideband (UWB) random noise radar technology is an ideal solution (Narayanan and Xu, 2003). The technique works by transmitting a random noise waveform and cross-correlating the reflected echoes with a time-delayed (to obtain range information) and frequency-shifted (to ensure phase coherence) replica of the transmit signal. Random noise signals are inherently difficult to detect and jam. Since UWB radars used for TWS applications are typically in the UHF range (250-750 MHz) for good penetration through walls and building materials, chip-based arbitrary signal generators can be used as noise sources and digital radio frequency memory (DRFM) technology can be used for time-delay implementation, thereby achieving a total digital radar solution. The 500-MHz bandwidth will yield an acceptable 30-cm (1-foot) range resolution. The major challenge is to develop a simplified architecture which will reduce cost without sacrificing performance. Preliminary simulations indicate that we can use 2-bit signal quantization which would permit more rapid range scanning by the DRFM (Xu and Narayanan, 2003). A typical system block diagram of the digital noise radar is presented in Fig. 1. Using two 1.5-GHz ADCs, the analog signals from the transmitter and receiver can be digitized independently and saved into the flash memory. A variable digital delay line is used for achieving transmit signal delay. In this architecture as depicted, we note that the entire received signal waveform after the antenna is digitized and saved into memory. Digital filtering, FFT, cross-correlation, and other signal processing can be done in real-time by the DSP chip or by the laptop computer. The current FPGA chips also provide high capabilities for real-time processing. By continually adjusting the operating parameters to dynamically adapt to the environment, we can obtain more accurate results and refine our data model more easily.

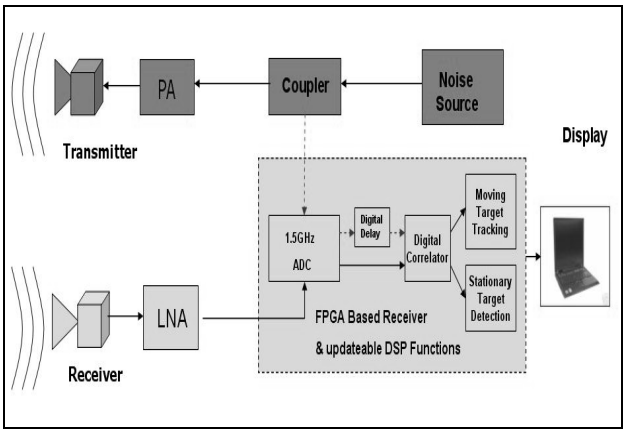

Fig. 1: Typical system block diagram of a digital noise radar. The digital correlator provides the cross-correlation between the time-delayed A/D-converted transmit waveform and the A/D-converted receive waveform.

2.2 Mathematical model

The digital noise radar system is an incoherent radar system which means the phase information is not used for target position detection. The advantage of this incoherent detection is a reduction in system complexity. Thus, I/Q detectors and mixers used for amplitude and phase detection are not needed, as used in a coherent noise radar described by Narayanan et al. (1998). A digital delay line can be formed using a computer memory in which the time-delayed replica of the transmit signal can be stored. The transmit noise waveform can be expressed as

$$X_t(t) = X_c(t)\cos(2\pi f_0 t) - X_s(t)\sin(2\pi f_0 t) \quad (1)$$

where X_c and X_s are the zero-mean Gaussian in-phase (I) and quadrature (Q) components and f_0 is the instantaneous center frequency (Dawood, 2001). The received signal $X_r(t)$ and the time-delayed transmit replica $X_d(t)$ can be expressed as, respectively,

$$\begin{aligned} X_r(t) = k_1\{ & X_c[(1+\alpha)t-\tau_0]\cos[2\pi f_0(1+\alpha)t-2\pi f_0\tau_0] \\ & - X_S[(1+\alpha)t-\tau_0]\sin[2\pi f_0(1+\alpha)t-2\pi f_0\tau_0]\} \end{aligned} \quad (2)$$

$$\begin{aligned} X_d(t) = \frac{1}{2}\{ & X_c[t-\tau_d]\cos[2\pi f_0 t - 2\pi f_0\tau_d] \\ & - X_s[t-\tau_d]\sin[2\pi f_0 t - 2\pi f_0\tau_d]\} \end{aligned} \quad (3)$$

where τ_d is the digital delay. If R is the range to the target which is moving with a velocity v_0, then the round-trip time delay is given by $\tau_0 = 2R/c$ where c is the velocity of wave propagation. The delay rate α is given by $\alpha = 2v_0/(c-v_0) \approx 2v_0/c$, and is practically zero for human motion. The cross-correlation between signals $X_r(t)$ and $X_d(t)$, assuming that $X_c(t)$ and $X_s(t)$ are

uncorrelated WSS processes and $\tau = \tau_d - \tau_0$, can be derived as

$$\Phi_{rd}(\alpha,t,\tau) = \frac{1}{2}k_1 E\{\Phi_{cc}(\alpha t+\tau)\cos[2\pi f_0(\alpha t+\tau)]\} \quad (4)$$

where $\Phi_{xy}(\cdot)$ denotes the auto or cross correlation function and $E\{\cdot\}$ denotes expected value. Note that the autocorrelation function in equation (4) is centered at f_0 and shows a peak when $\tau = 0$, i.e., when $\tau_0 = \tau_d$. Thus, measurement of the appropriate delay provides target range information.

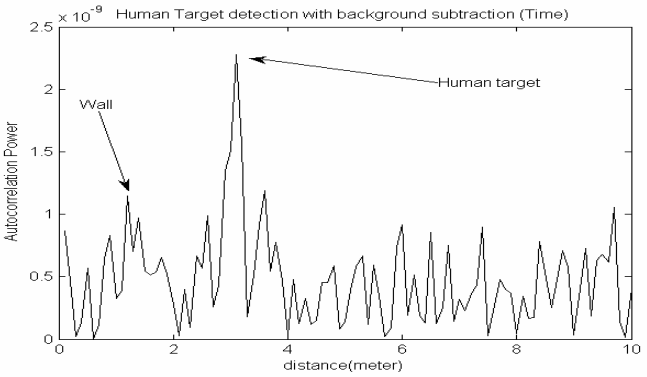

Fig. 2: Wall and human position as observed by a non-coherent random noise radar.

A simulation study was performed in order to locate a human at a distance of 2 m behind a brick wall of thickness 50 cm using the non-coherent noise radar technique described above. The dielectric constants of brick and human were assumed to be 9 and 81 respectively. From Fig. 2, we can clearly see that there are two peaks at ranges of 1 m and 3 m. The first peak yields the position of the front of the wall and the second peak yields the position of the human. Of course, both peaks look alike and thus this technique can only detect the presence of a target at a particular range without being able to recognize or identify a human from the data. From Fig. 2, we can also see other interference peaks and they are not small compared to the peak of human target. When the human target moves toward the back wall, the human target reflection will getting smaller and the false alarm will increase.

3. SIGNAL DETECTION BEHIND THE WALL

Before we start the radar system design, the first work is to simulate the radar system performance according to different parameters. The finite difference time domain (FDTD) is a popular method to simulate UWB propagation through walls but it has limited ability to develop the radar signal processing based on our need. One of the SDR concepts is to incorporate MATLAB® code in real FPGA implementation. Our through wall radar development is also based on our MATLAB® based simulator and it has following characteristics.

(i) Transmitter power, waveform frequency and bandwidth can be separately controlled.
(ii) Material, width, transmission coefficients and reflection coefficients of the wall are adjustable. The interference of clutters and thermal noise can be added.
(iii) Microwave through wall propagation is based on ray tracing technology.
(iv) Radar signal processing and position tracking can be presented in the simulator. Those signal processing algorithms can be realized on FPGA through the Xilinx system generator or programmed by VHDL.

The receiver performance can be analyzed at the simulator output based on detection and estimation theory (Srinath et al., 1996). The radar system performance analyses are based on transmitter power, wall material, and antenna beamwidth.

3.1 Signal detection in the interference

Target detection is the main function of a radar system. Detection occurs when the radar decides on the presence or absence of an object or target. This paper uses the Neyman-Pearson criterion to derive the probability of false alarm P_F and probability of detection P_D. In order to find the probabilities of false alarm and detection, a hypothesis must be created and a likelihood ratio test (LRT) must be performed.

Hypothesis H_0 representing the presence of the noise, is formed as the subtraction of the stationary interferences with average background noise, given by equation (5). Stationary interferences include indoor multipath, coupling noise, thermal noise and clutter reflections. All the stationary interferences are assumed to be uncorrelated and Gaussian noise in (5) and (6). Hypothesis H_1 representing the presence of a human, is also formed as the summation of the human body reflections and noise in (7).

$$Z_{Avg\_Background\_Noise} = \overline{Y_{Coupling} + Y_{Wall} + Y_{clutters} + V_{Noise}} \quad (5)$$

$$\begin{aligned} H_0 : Z &= Z_{Instant\_No\_Target} - Z_{Avg\_Background\_Noise} \\ &= \left(Y_{coupling} + Y_{Wall} + Y_{Clutters} + V_{Noise}\right) - \left(\overline{Y_{Coupling} + Y_{Wall} + Y_{clutters} + V_{Noise}}\right) \\ &= Y_{NOISE} \end{aligned} \quad (6)$$

$$\begin{aligned} H_1 : Z &= Z_{Instant\_With\_Target} - Z_{Ag\_Background\_Noise} \\ &= \left(Y_{Human} + Y_{coupling} + Y_{Wall} + Y_{Clutters} + V_{Noise}\right) - \left(\overline{Y_{Coupling} + Y_{Wall} + Y_{clutters} + V_{Noise}}\right) \\ &= Y_{Human} + Y_{NOISE} \\ &= Y_{HUMAN} \end{aligned} \quad (7)$$

Hypotheses (6) and (7) are somewhat different than the detection examples in Srinath et al. (1996). Both return signals, Y_{Human} and Y_{NOISE}, are Gaussian random noise with almost the same mean and variance. It means that the signals in equations (6) and (7) have the same probability distribution function (PDF). If we take the likelihood ratio test (LRT), the threshold is close to unity and a non-practical result is generated. The efficient way to detect the different objects in the noise environment is to use the autocorrelation function. If the largest peak value appears at the center of the autocorrelation signals, it will be at the same time delay as the delayed signal $X_d(t)$. We can thus know the position of different objects by comparing the peak values. The question is how to define the PDF of the peak values of human and noise. Both peak values of noise (Y_{NOISE}) and human (Y_{HUMAN}) are also random but we do not know their distribution. If we have adequate data for both these peak values, we can plot their histograms. From Fig. 3, we can see that the histogram shapes are similar to a Gaussian and thus we can assume a Gaussian noise model for their PDF functions. From the simulation results, we can calculate the mean and variance of both signals. Equations (8) and (9) show Y_{NOISE} and Y_{HUMAN} distributed normally under each hypothesis.

$$p(\mathrm{z}\mid \mathrm{H}_0)=\prod_{i=1}^{N}\frac{1}{\sqrt{2\pi\cdot\sigma_{NOISE}{}^2}}\exp\left(\frac{-(z_i-m_{NOISE})^2}{2\cdot\sigma_{NOISE}{}^2}\right) \quad (8)$$

$$p(\mathrm{z}\mid \mathrm{H}_1)=\prod_{i=1}^{N}\frac{1}{\sqrt{2\pi\cdot\sigma_{Human}{}^2}}\exp\left(\frac{-(z_i-m_{Human})^2}{2\cdot\sigma_{Human}{}^2}\right) \quad (9)$$

A likelihood ratio can then be formed as follows:

$$\Lambda(z)=\frac{\prod_{i=1}^{N}\frac{1}{\sqrt{2\pi\cdot\sigma_{Human}{}^2}}\exp\left(\frac{-(z_i-m_{Human})^2}{2\cdot\sigma_{Human}{}^2}\right)}{\prod_{i=1}^{N}\frac{1}{\sqrt{2\pi\cdot\sigma_{NOISE}{}^2}}\exp\left(\frac{-(z_i-m_{NOISE})^2}{2\cdot\sigma_{NOISE}{}^2}\right)}\underset{H_0}{\overset{H_1}{\gtrless}}\gamma \quad (10)$$

According to the observation results, the variances of wall and human reflections are almost the same. Equation (10) can be recast as follows, where γ^+ is the new threshold.

$$\sum_{i=1}^{N}z_i\underset{H_0}{\overset{H_1}{\gtrless}}\frac{2\sigma^2{}_{NOISE}\cdot\ln\gamma+\left(m^2{}_{NOISE}-m^2{}_{Human}\right)}{2\cdot(m_{NOISE}-m_{Human})}=\gamma^+ \quad (11)$$

Probabilities P_F and P_D are calculated as the following integrals in equations (12) and (13).

$$P_F=\int_{r^+}^{\infty}p(\mathrm{z}_{\mathrm{NOISE}}|\mathrm{H}_0)=\int_{r^+}^{\infty}\prod_{i=1}^{N}\frac{1}{\sqrt{2\pi\cdot\sigma_{NOISE}{}^2}}\exp\left(\frac{-(z_i-m_{NOISE})^2}{2\cdot\sigma_{NOISE}{}^2}\right) \quad (12)$$

$$P_D=\int_{r^+}^{\infty}p(\mathrm{z}_{\mathrm{Human}}|\mathrm{H}_1)=\int_{r^+}^{\infty}\prod_{i=1}^{N}\frac{1}{\sqrt{2\pi\cdot\sigma_{Human}{}^2}}\exp\left(\frac{-(z_i-m_{Human})^2}{2\cdot\sigma_{Human}{}^2}\right) \quad (13)$$

In radar target detection, the concept of constant false alarm rate (CFAR) is widely used. A CFAR detector need not be optimal, but it does have to provide the require false alarm rate under this assumption. The constant false alarm rate is used to obtain the suitable detection threshold using the following expression:

$$\alpha=P_F=\int_{r^+}^{\infty}p(\mathrm{z}_{\mathrm{NOISE}}|\mathrm{H}_0)=\int_{r^+}^{\infty}\prod_{i=1}^{N}\frac{1}{\sqrt{2\pi\cdot\sigma_{NOISE}{}^2}}\exp\left(\frac{-(z_i-m_{NOISE})^2}{2\cdot\sigma_{NOISE}{}^2}\right) \quad (14)$$

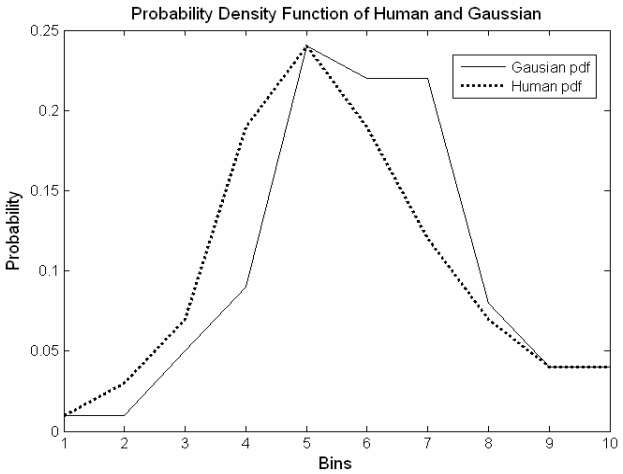

Fig. 3: Histograms of peak values for human reflection and noise.

3.2 Effects of transmit power (dynamic range)

The measure of radar's performance is captured in its receiver operating characteristics (ROC) which relates its detection probability to its false alarm probability. Using equations (12) and (13), we can generate the ROC curves. Generally, if we want to improve the detection probability, we can increase the transmitter power. This means that its signal-to-interference ratio (SIR) will also increase. Results of a simulation performed at different transmitter power levels are depicted in Fig. 4 (human at 2 meter, wall at 0.5 meter, interference level at -65 dBm). The curve moves slightly upward with increasing transmitter power, although the improvement may not justify the expense of the higher power. However, when the transmit power spectral density

(PSD) exceeds -30 dBm/MHz, the performance improvement starts to saturate. In general, we note that the ROC curve appears promising, and the false alarm probability is less than 0.2 (20%) for a detection probability of 0.8 (80%) even at a transmit PSD of -70 dBm/MHz. The maximum PSD of a UWB transmitter is +15 dBm/MHz based on FCC limitations. That means the maximum dynamic range our radar can achieve is 85 dB. Since the distances within a room are not too high, we limit the transmit power of this radar to -20 dBm; thus, we still have a 50-dB dynamic range that can detect the moving target at a distance of 37 meter in front of the radar with few false alarms. In the real world, the actual dynamic range is much less than this value because the interference is much higher.

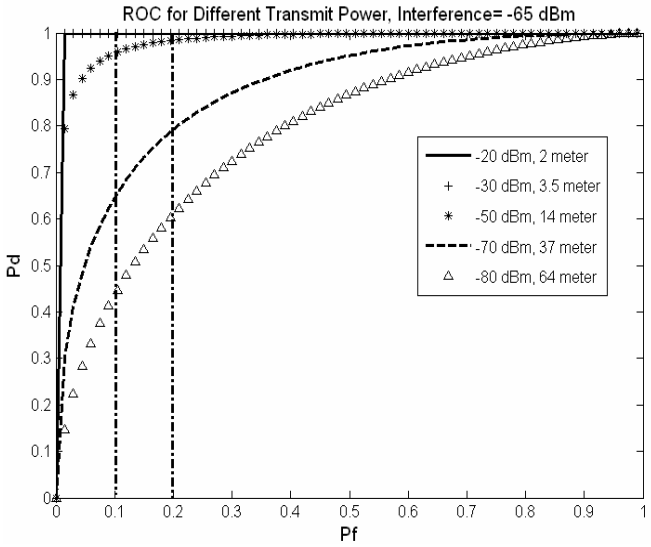

Fig. 4: ROC curves for different transmitter power levels. The human is at 2 m and the wall at 0.5 m from the radar.

3.3 Effects of wall dielectric constants

The wall dielectric constant is another important parameter that affects through-wall sensing. Metal walls are fully reflective and thus detection through such walls is impossible using radar. However, most wall materials in use are wood, concrete, glass, and stone. We simulated several of the above materials and ROC curves are shown in Figure 5 (a) and (b). In Fig. 5 (a), we can not find the effects of different wall materials because the strong reflections from the human body at two meter dominate the receiver performance. But we do find that the material dielectric constant affect the detection performance when human is far away from the wall. The higher the dielectric constant, higher is the wall reflectivity, and thus lower is the energy transmitted through to the inside. In most cases, unless the walls are wet, one can achieve a false alarm probability of 0.2 (20%) for a detection probability of greater than 0.95 (95%).

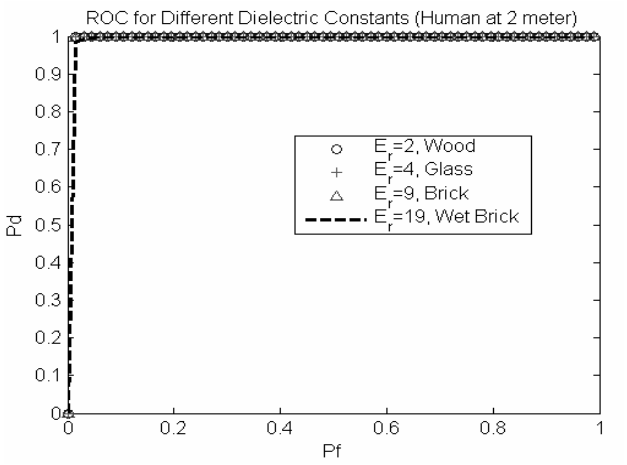

(a) Human at 2-m distance.

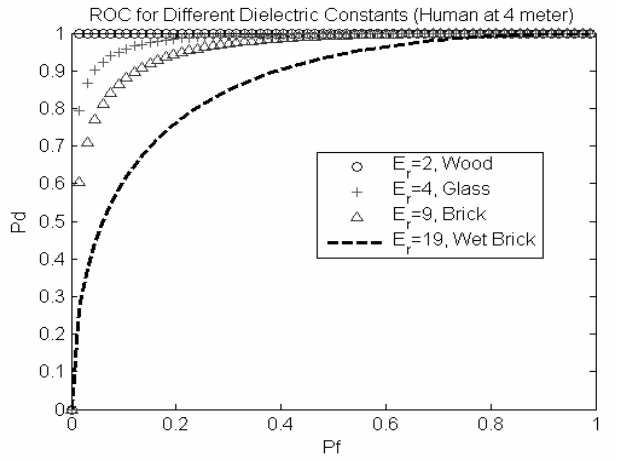

(b) Human at 4-m distance.

Fig. 5: ROC curves for different wall dielectric constants.

3.4 Effects of antenna half power beamwidth

In order to minimize the noise and increase the human reflection in the interference, use of beamforming technology is one solution. If the antenna beamwidth is narrow, it is easy to pick up the line of sight signals but not out of sight interferences. The gain of the antenna will also increase and sidelobe energy is suppressed. Due to limitations of larger antenna size and weight in the low frequency range, beamforming is hard to realize in real applications. However, we still present the effects of different antenna beamwidths. Fig. 6 (a) and (b) show the human target detection with different beamwidths. The background noise in Fig. 6(a), which has a narrower beamwidth, is smaller than in Fig.6 (b) which has a wider beamwidth. Fig. 7 is the ROC plot of four different beamwidths when human target is 4.5 m behind the wall. We can clearly see the beamwidth 100° has the worst performance and the beamwidths less than 60° have much better performance. According to the design experience, if the gain of the antenna is greater than 6 dB, its beamwidth is less than 60°.

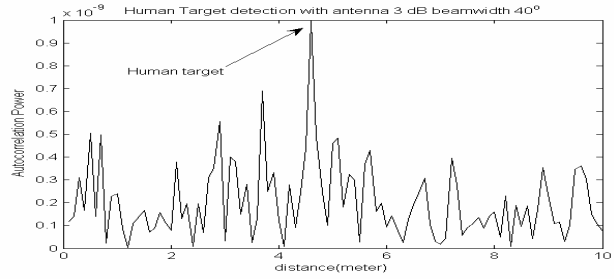

(a) 3-dB beamwidth = 40°

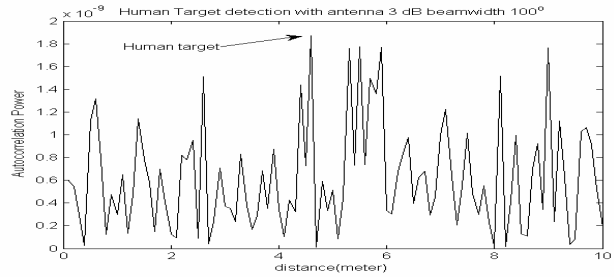

(b) 3-dB beamwidth = 100°

Fig.6: Human target detection for different beamwidths.

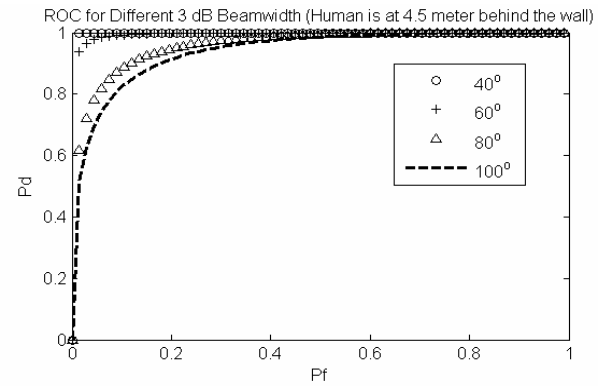

Fig.7: ROC curves for different 3-dB beamwidths.

4. EXPERIMENTAL RESULTS

4.1 Experiment setup

The through wall radar test is conducted in a standard classroom (12 m × 6 m). The wall material of the classroom is concrete and its thickness is 30 cm. The radar system is shown in Fig. 8(a) and the experimental setups are in Fig. 8(b). In order to present the usual situation in the room, we pick up the classroom which is not empty and it has a lot clutters in the room, shown in Fig. 8(c). Background reflected signals are first recorded as a reference signal. The backscattering signals of human in the classroom will be subtracted with the previous reference signal, shown in Fig. 8(d). The real-time transmit and receive signals are shown in Fig. 9(a) and their power spectra in Figs. 9(b) and 9(c). The radar system uses two identical wideband directional antennas. The gain of the antenna is 6 dB and its bandwidth is 350 MHz-1000 MHz. The radar's RF components include a noise generator, a low pass filter, a power amplifier and a low noise amplifier.

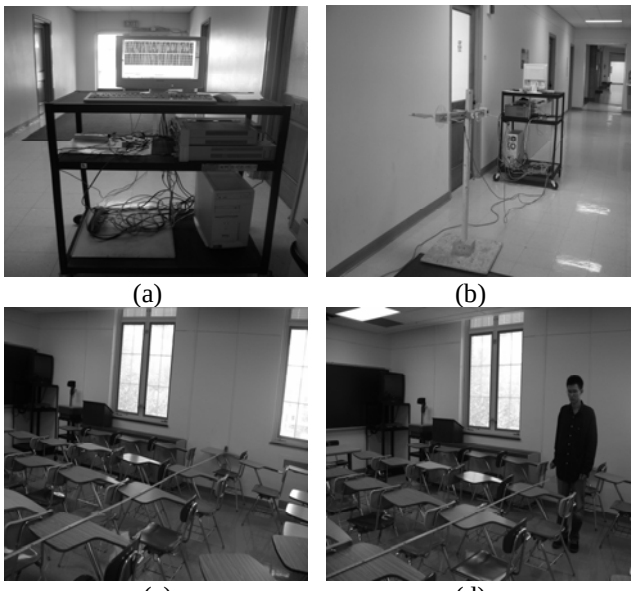

(a) (b)

(c) (d)

Fig. 8: (a) Radar system setup; (b) Field test; (c) Background; (d) Human in the room.

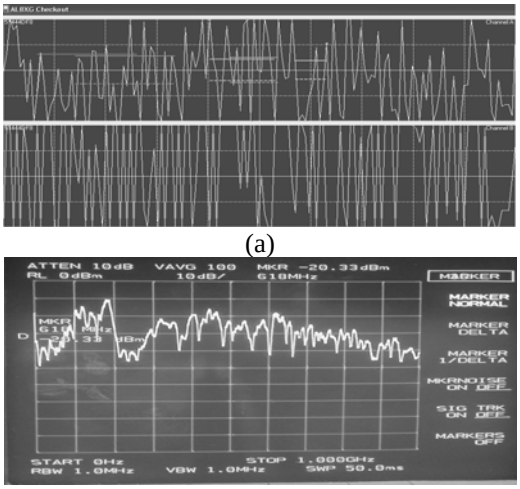

(a)

(b)

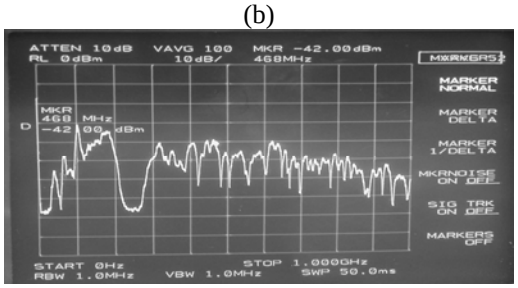

(c)

Fig. 9: (a) Real-time transmit signal (top) and receive signal (bottom); (b) Power spectrum of the transmit signal; (c) Power spectrum of the receive signal.

4.2 Single human detection

Although data subtraction is a conventional method to remove the interference, it is effective for real-time monitoring. This method suffers from the noise residue problem when target signal is very weak compared to the interference. The strong noise residues produce a lot of false alarms when the human target is moving farther than 4 m, as shown in Fig. 10. The ROC of the single human detection is plotted in Fig.11. When the human distance is less than 3 meter behind the wall, the result is very close to the simulation results of Fig. 4. When the human distance is further than 3 m, the performance is not as good as simulation results. If we look at the human target at 6 m distance in Fig.11, the curve is close to the -70 dBm curve in Fig. 4, which can detect the human at 37 m. But from the radar range equation, the reflected power from the human body at 6 m should be -39 dBm (19-dB loss). There is a 31-dB difference between simulation and measurement.

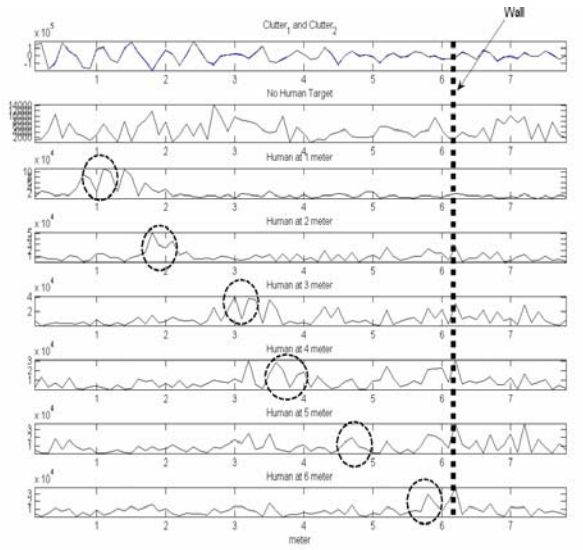

Fig. 10: Human target movement from 1 m to 6 m.

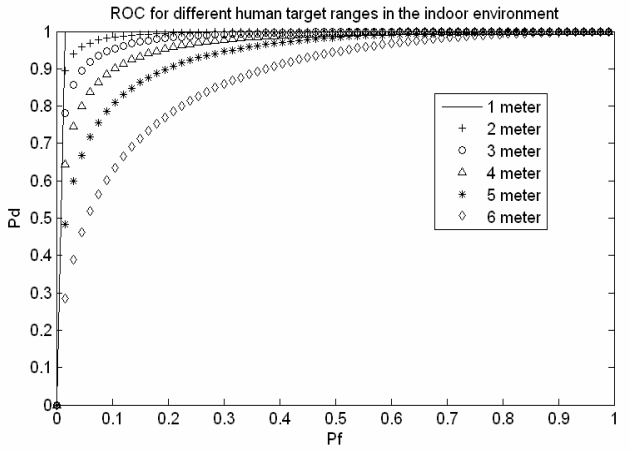

Fig. 11: ROC curves for human target movement from 1 m to 6 m.

The factors that cause unsatisfactory performance include indoor clutter, antenna coupling, and multipath. If the antenna beamwidth is wider, the transmitted energy diverges quickly with range and the antenna easily picks up the interference. In Section 3.4, we concluded that beamforming technology can improve the receiver performance. Also from the simulation study, we learned that the detection performance worsens when the transmit power is lower than 10 dB below the interference. If we can correctly estimate the interference power, the simulation will be matched better to the measurement results. In Fig. 12, if we increase the interference level from -65 dBm to -34 dBm (i.e., add 31 dB), the simulation result is seen to match the measurement results, but the receiver dynamic range is only 20 dB according to CFAR ($P_d = 80\%$ and $P_f = 20\%$).

Increasing the correlation length and the averaging more samples will improve the SIR. The cost, however, is the time lag for real-time data processing. We believe, therefore, that adaptive beamforming can better suppress the interference and improve the detection performance.

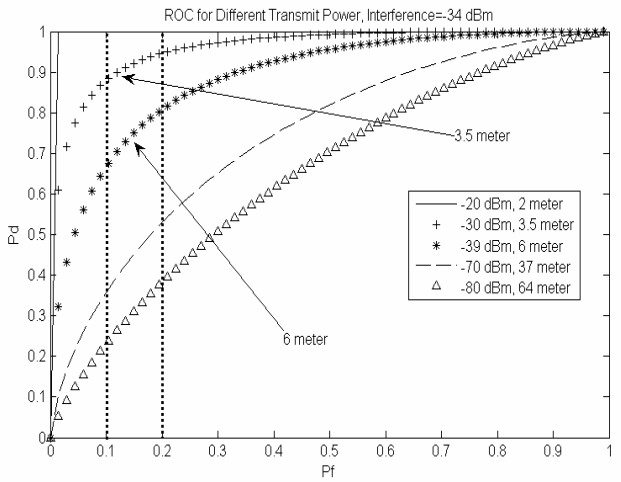

Fig. 12: ROC curves for different transmitter power levels. The human is at 2 m and the wall at 0.5 m from the radar.

4.3 Multiple human detection

In order to detect the movements of multiple persons in the room, the radar system needs to have high range resolution. Our radar system has a 400-MHz bandwidth and the ideal range resolution is 37.5 cm. In this experiment, we placed two humans in different locations inside the room. First, both humans were 1 m apart from each other. We can clearly see two peaks at 2.5 m and 3.5 m distances in Fig. 13. Next, we moved both humans closer to each other, i.e., 50 cm apart. We still can see two peaks at 3.2 m and 3.6 m distances. The measurement error comes from the sampling rate of high speed ADC. A 1.5-GHz sampling rate will give ±10-cm sampling error. If we can increase the sampling rate of the high speed ADC, we can sample at a higher frequency yielding better range resolution and lower sampling error.

The state-of-the-art single ADC can sample as high as 2.2 GHz and gives finer range resolution.

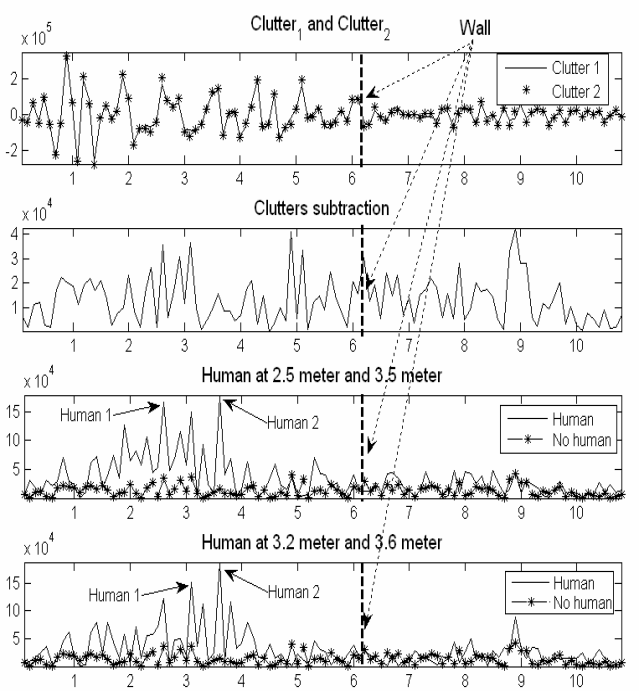

Fig. 13: Two human targets movement location.

4.4 Summary of the UWB random noise radar system

Table 1 summarizes the performance characteristics of our radar system. All the parameters are based on actual measurement and correspond to the theory. The advanced portable system can be realized easily based on the prototype system design.

TABLE 1: CHARACTERISTICS OF RADAR SYSTEM

Parameter	Value
Frequency	350 MHz – 750 MHz
Transmit PSD	-20 dBm/MHz
Total Radiated Power	4 mW
Polarization	HH
Antenna Gain	6 dB
ADC	8 Bits
Sampling Rate	1.5 GHz/per channel
Dynamic Range (0.8 P_d; 0.2 P_f)	20 dB
Range Resolution	40 cm
Maximum Receive Power	+30 dBm

CONCLUSIONS

The results presented in this paper show that noise radars are useful for detecting and tracking moving humans obscured by building walls. The technique works by cross-correlating the received signal with a time-delayed replica of the transmit waveform. The noise waveform has excellent properties such as low cost of generation, immunity to interference and jamming, low probability of intercept, and low probability of detection. The LPI and LPD properties make the waveform attractive for covert detection, tracking, and imaging applications to confound today's techno-terrorists. Additional studies are underway to develop better signal processing algorithm to improve the SIR and new beamforming technology to minimize the clutter fading. We believe that these improved techniques will translate into better ROC for robust detection of human motion behind walls.

REFERENCES

Dawood, M., 2001: *Ultrawideband Coherent Random Noise: Theory and Experiments*, Ph.D. dissertation, University of Nebraska, Lincoln, NE.

Nag, S., and Barnes, M., 2003: A moving target detection filter for an ultra-wideband radar, *Proceedings of the IEEE Radar Conference*, Huntsville, AL, 147-153.

Narayanan, R.M., and Xu, X., 2003: Principles and applications of coherent random noise radar technology, *Proceedings of the SPIE Conference on Noise in Devices and Circuits*, Santa Fe, NM, 503-514.

Narayanan, R.M., Xu, Y., Hoffmeyer, P.D., and Curtis, J.O., 1998: Design, performance, and applications of a coherent ultrawideband random noise radar, *Optical Engineering*, **37**, 1855-1869.

Narayanan, R.M., Xu, X., and Henning, J.A., 2004: Radar penetration imaging using ultra wideband (UWB) random noise waveforms, *IEE Proceedings on Radar, Sonar and Navigation*, **151**, 143-148.

Popovic, M.A., Chan, K.H., and Lin, J.C., 1984: Microprocessor based non-contact heart rate/respiration monitor, *Proceedings of the International Conference of IEEE Engineering in Medicine and Biology Society*, Los Angeles, CA, 754-757.

Srinath, M.D., Rajasekaran, P.K., and Viswanathan, R., 1996: *Introduction to Statistical Signal Processing with Applications*. Upper Saddle River, NJ: Prentice Hall.

Tsui, J.B., 1989: *Digital Techniques for Wideband Receivers.* Boston, MA: Artech House.

Wiesbeck, W., 2001: SDRS: software-defined radar sensors, *Proceedings of the IEEE International Geoscience and Remote Sensing Symposium*, Sydney, Australia, 3259-3261.

Wu, Y., and Li, J., 1998: The design of digital radar receivers, *IEEE Aerospace and Electronic Systems Magazine*, **13** (1), 35-41.

Xu, X., and Narayanan, R.M., 2003: Impact of different correlation receiving techniques on the imaging performance of UWB random noise radar, *Proceedings of the IEEE International Geoscience and Remote Sensing Symposium*, Toulouse, France, 4525-4527.